

EXPLORING THE LIMITS OF HIGH ALTITUDE GPS FOR FUTURE LUNAR MISSIONS

Benjamin W. Ashman*, Joel J. K. Parker[†], Frank H. Bauer[‡], and Michael Esswein[§]

An increasing number of spacecraft are relying on the Global Positioning System (GPS) for navigation at altitudes near or above the GPS constellation itself—the region known as the Space Service Volume (SSV). While the formal definition of the SSV ends at geostationary altitude, the practical limit of high-altitude space usage is not known, and recent missions have demonstrated that signal availability is sufficient for operational navigation at altitudes halfway to the moon. This paper presents simulation results based on a high-fidelity model of the GPS constellation, calibrated and validated through comparisons of simulated GPS signal availability and strength with flight data from recent high-altitude missions including the Geostationary Operational Environmental Satellite 16 (GOES-16) and the Magnetospheric Multiscale (MMS) mission. This improved model is applied to the transfer to a lunar near-rectilinear halo orbit (NRHO) of the class being considered for the international Deep Space Gateway concept. The number of GPS signals visible and their received signal strengths are presented as a function of receiver altitude in order to explore the practical upper limit of high-altitude space usage of GPS.

INTRODUCTION

Recent years have seen a renewed interest in lunar exploration, both as a target for in-situ rovers and landers (such as India’s Chandrayaan-2¹ and China’s Chang’e 4/5²), and as a first step toward deep-space human exploration, with NASA’s Exploration Mission 1 (EM-1) and Exploration Mission 2 (EM-2).³ In early 2017, NASA and other space agencies announced the international Deep Space Gateway (DSG),⁴ a project to “build a crew tended spaceport in lunar orbit [...] that would serve as a gateway to deep space and the lunar surface.” That December, the president of the United States issued Space Policy Directive 1, calling for a “return of humans to the Moon for long-term exploration and utilization, followed by human missions to Mars and other destinations”.⁵

Navigation for lunar-vicinity spacecraft has conventionally been performed on the ground, using measurements from ground-based radiometric ranging facilities. But recent developments in the field of autonomous, on-board navigation increasingly allow spacecraft to calculate their own navigation solutions in real-time, greatly increasing spacecraft responsiveness, reducing the burden on ground-based tracking networks, and cutting overall mission costs. Autonomous, on-board navigation using the Global Positioning System (GPS) has developed rapidly over the past two decades.

* Aerospace Engineer, Code 595, NASA Goddard Space Flight Center, Greenbelt, MD

[†] Aerospace Engineer, Code 595, NASA Goddard Space Flight Center, Greenbelt, MD

[‡] FBauer Aerospace Consulting Services, Silver Spring, MD

[§] Virginia Polytechnic Institute, Blacksburg, VA

Numerous studies have been performed in that time regarding the use of GPS as a component in a lunar-distance navigation architecture. This paper presents a simulation of GPS signal availability for a lunar mission, leveraging the experiences of recent high altitude missions employing GPS operationally, Geostationary Operational Environmental Satellite 16 (GOES-16) and the Magnetospheric Multiscale (MMS) mission. While signal availability is only a component of a full, mission-level, navigation design study, this paper seeks to establish a signal visibility baseline supported by flight data to contribute to future mission-specific work.

BACKGROUND

Use of Global Navigation Satellite System (GNSS) signals for on-board autonomous navigation of spacecraft has become ubiquitous on spacecraft in Low Earth Orbit (LEO)—those missions defined as below 3000 km in altitude. As this technique began to grow and mature and the tremendous advantages of real-time on-board navigation became evident, expansion to employ GPS for navigation in High Earth Orbit (HEO), in Geostationary Earth Orbit (GEO), and beyond became the next technological challenge.

Several GPS signal experiments flown in the late 1990s and early 2000s incrementally provided a more comprehensive understanding of the capabilities and limitations of high-altitude GPS navigation. Early flight experiments demonstrated basic feasibility (e.g., Equator-S,⁶ Falcon Gold⁷) and orbit determination at GEO,⁸ and in 2001 the AMSAT OSCAR-40 (AO-40) experiment mapped the visible GPS main and sidelobe signals.^{9,10} This data supported the formal Space Service Volume (SSV) definition in 2006,¹¹ and additional flight experiments have been performed as international GNSS constellations have been established.^{12,13} The SSV represents the volume of space surrounding the Earth from the edge of LEO to GEO, defined for these purposes as 3000 km to 36,000 km. As shown in Figure 1 the SSV overlaps and extends beyond the constellation itself, so utilization of GNSS signals in this region often requires signal reception from GNSS satellites on the opposite side of Earth. As a result, signal availability is hampered by poor geometry, signal occultation by the Earth itself, and weaker signal strength.¹⁴

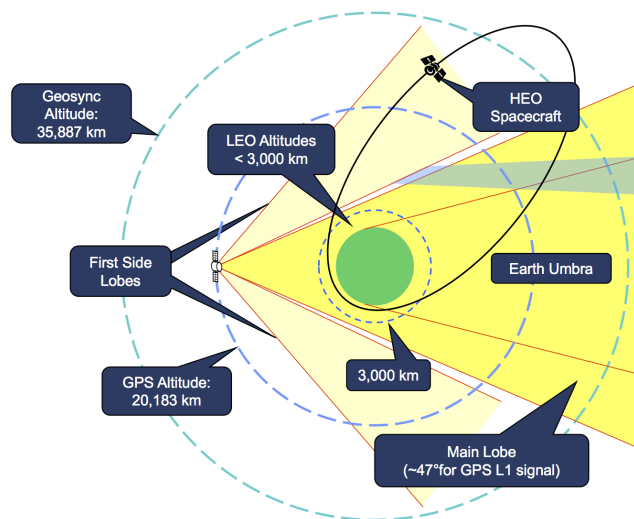


Figure 1. Geometric view of GNSS signal use in space. The SSV is defined as 3,000 km to 36,000 km altitude.

Building on this flight data, weak signal receiver¹⁵ and high gain antenna technology advanced to address signal strength issues in the SSV, leading to NASA's first operational deployments of high-altitude GPS navigation. The first of these, the MMS mission, was launched in 2015, followed closely by the GOES-16 spacecraft in 2016. Operational data from MMS unveiled the full capability of GPS within the SSV and up to 76,000 km,¹⁶ substantially extending SSV performance knowledge with a continuous data set containing the full data triad necessary to understand and accurately simulate GPS in the SSV and beyond: signal availability, signal strength, and estimated position accuracy. In 2017, additional data at GEO was published in 2017 from initial operations of the GOES-16 spacecraft,¹⁷ and MMS apogee raising maneuvers further extended the dataset to 150,000 km - 40% of the way to the Moon.¹⁸ Figure 2 depicts the GPS high altitude operational missions (solid bars) and past flight experiments (striped bars).

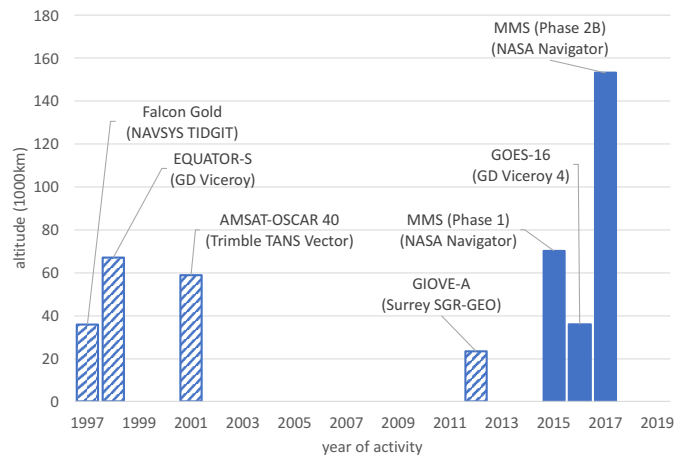


Figure 2. High Altitude GPS Missions.

A concept to employ GPS for lunar missions was developed and presented as early as 1993.¹⁹ This concept considered using GPS to support lunar arrival and departure, and proposed employing a pseudolite constellation orbiting the moon for lunar orbit and surface operations. Shortly after the AO-40 data set was unveiled, NASA embarked on a new Vision of Space Exploration—to take humans beyond LEO, to the moon, and ultimately to Mars. These two independent events resulted in a flurry of papers investigating the feasibility and limitations of GPS navigation in cislunar space. Carpenter²⁰ (2004) investigated the use of GPS and a single Earth-Moon Libration-2 orbiter to support missions in cislunar space. Bamford²¹ (2008) and Winternitz²² (2009) analyzed the use of the NASA Goddard Space Flight Center (GSFC) Navigator receiver for lunar missions, demonstrating that it could support the critical phases of ascent, entry, and lunar return. Lee²³ (2009) investigated the use of GPS exclusively for navigation during a lunar Earth return trajectory on NASA's Orion human spaceflight capsule, concluding that a weak signal receiver and high gain GPS antenna could improve navigation performance during critical final phases of flight. Witternigg²⁴ (2015) performed simulations of a loosely coupled GNSS-Inertial Navigation System employing GPS and Galileo, concluding that GNSS could improve the robustness and autonomy of future exploration missions. Several other studies looked at GNSS availability with ever-improving information from GNSS on-orbit and antenna pattern data, Capuano²⁵ (2015), Shehaj²⁶ (2017). Most recently, Winternitz¹⁸ (2017) used the data obtained from MMS and the GSFC Navigator GPS receiver to extrapolate GPS performance at lunar distance.

The goal of this simulation is to apply the most accurate on-orbit GPS constellation model available in order to derive potential achievable real-world performance at high altitude. Previous studies have considered representative or minimum-specification constellations, or were performed before the wide availability of accurate and high-fidelity ground-based measurements of the GPS antenna patterns.

SIMULATION

GPS signals are considered visible if an unobstructed line of sight exists between the transmitting GPS satellite and the GPS antenna on the user spacecraft, and the received signal power exceeds the receiver’s acquisition or (if already acquired) tracking threshold. Received signal carrier-to-noise spectral density (C/N_0) is simulated according to the link budget

$$C/N_0 = P_T + A_d + G_T + G_R - (T_s + k + Nf), \quad (1)$$

where P_T is the transmitted power, A_d is the free space path loss, G_T and G_R the gains of the transmit and receive antennas respectively, T_s the system noise temperature, k Boltzmann’s constant, and Nf the noise figure of the receiver and low noise amplifier (LNA). This link is computed for each GPS satellite using Orbit Determination Toolbox (ODTBX), a mission simulation and analysis tool developed in MATLAB by engineers at GSFC.²⁷ ODTBX is a collection of scripts that simulates all of the ingredients to compute Equation (1): user antenna pattern and relevant receiver properties, relative geometry of the GPS constellation and user spacecraft, and transmitted power and antenna gain patterns for each of the individual GPS satellites.

GPS Constellation Model

GPS was the focus of the current simulation, so no additional GNSS constellations or augmentations were modeled. Likewise, we focused only on the L1 Coarse Acquisition (C/A) signal, which is the primary signal used for spacecraft navigation currently and in the near future. The modernized L1C, L2C, and L5 signals may offer significant benefits for certain use cases, but are not currently used operationally in onboard spacecraft navigation.

The GPS constellation model chosen for this analysis was the actual on-orbit constellation during the flight missions used for simulation verification—the constellation make-up did not change between March 30th and May 22nd 2017, the GOES-16 and MMS epochs, respectively. The lunar simulation was analyzed at the MMS epoch rather than an epoch expected for such a mission (e.g., 2020) in order to avoid error in time-shifting the GPS constellation model. The on-orbit configuration of the constellation at this epoch is shown in Table 1.

The constellation used consisted of 31 Space Vehicles (SVs), with 8 of Block IIR design, 4 of Block IIR design with the modernized IIR-M antenna panel, 7 of Block IIR-M design, and 12 of Block IIF design. In the case of the IIR and IIR-M SVs, we used the ground-test antenna gain measurements released publicly by Lockheed Martin.²⁸ In the case of the IIF SVs, no public ground-test data is available. The IIF antenna gain pattern is known to be similar to that of the Block IIA SVs, which does have a publicly-available 1-dimensional pattern available to 65 deg elevation angle,²⁹ or off-boresight, so this was used instead of the actual IIF gain data. Figure 3 illustrates the patterns used. For simplicity, the average over azimuth is shown for each pattern in this figure, though the simulation uses the entire 2D pattern for IIR and IIR-M. For the transmit power, in all cases minimum values were used that meet the GPS edge-of-Earth received power specification, as described by Parker³⁰ (2016).

Table 1. GPS constellation configuration.

Block	IIR	IIR*	IIR-M	IIF
Number of SVs	8	4	7	12
SVs	41, 43–46, 51, 54, 56	47, 59, 60–61	48, 50, 52–53, 55, 57–58	62–73
TX antenna pattern	GPS IIR, 0–90° el coverage, spacing: 2° el, 10° az,	GPS IIR-M, 0–90° el coverage, spacing: 2° el, 10° az	GPS IIR-M, 0–90° el coverage, spacing: 2° el, 10° az	GPS IIA (1D), 0–65° el coverage, 1° el spacing
TX transmit power	13.5 dBW	12.8 dBW	12.8 dBW	12.8 dBW

IIR* refers to Block IIR SVs with the modernized IIR-M antenna panel.

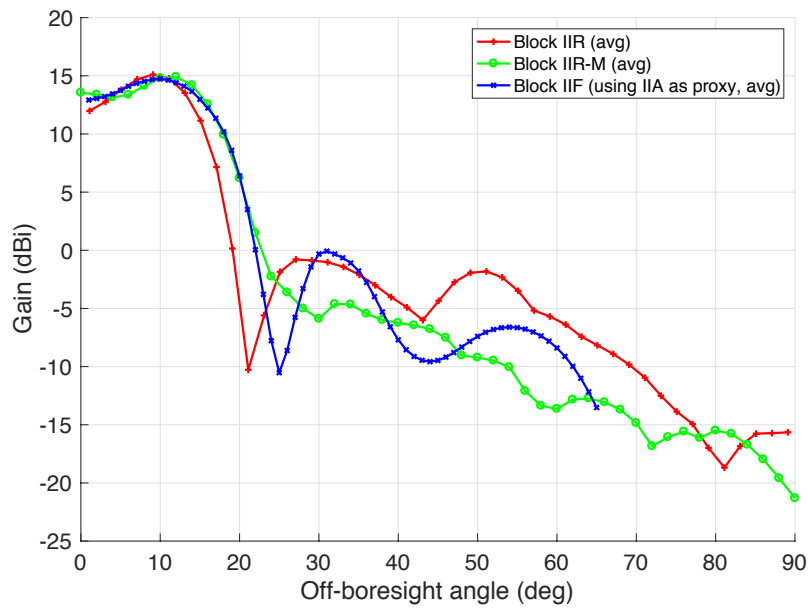


Figure 3. GPS constellation model transmit antenna patterns.

We used the YUMA almanac files associated with the simulation times in each case to establish the GPS satellite orbits and healthy status. Unhealthy or missing satellites were not considered, as was the case with PRN 4. SV attitude was modeled according to the standard Bar-Sever attitude model.³¹

Verification With GOES-16 Flight Data

GOES-16 is the first operational use of GPS for a US civilian GEO satellite. Stringent navigation requirements during and after maneuvers require that the GPS receiver be able to acquire and track sidelobe signals.³⁰ Successful on-orbit performance of the GPS receiver was demonstrated in early 2017, with more than 11 GPS satellites typically incorporated into the position, velocity, and timing (PVT) solution, and no outages.¹⁷ This is a mission operating at the formal limit of the SSV, sensitive to the details of the GPS sidelobes. Here we compare simulated GPS signal availability to flight data as a means of validating the GPS constellation model and other elements of the ODTBX simulation.

We simulated a 27 hour span, slightly more than one orbit, beginning at 18:00 UTC on March 30, 2017. The GOES-16 GPS antenna is specially designed for receiving sidelobes, with a peak gain of 11 dB at 22° off-boresight and a half-beamwidth of 40°. We used a definitive ephemeris and modeled the 12-channel GPS receiver with an acquisition and tracking threshold of 25 dB-Hz—this was chosen according to the flight data by inspection, though tracking has been demonstrated down to 17 dB-Hz.¹⁷

Intervals when each SV was visible over the duration of the simulation are shown in Figure 4, with flight data results overlaid in black. The simulation and flight data generally agree, with an average of 11.8 satellites visible in the simulation case and 11.2 in the flight data. However, the flight data exhibits more outages than the simulation. To study this further, C/N_0 values for three representative SVs is shown in Figure 5. Although the main lobes are accurately captured, some of the detail of the sidelobes is missed. Block IIF SVs in particular are responsible for many of the cases where outages in the flight data are not reflected in the simulation. This is the only block for which an azimuthally averaged pattern is used; Shehaj²⁶ (2017) showed that ignoring azimuthal variation does not significantly impact the number of SVs visible over time, but it does fail to capture momentary outages, impacting navigation.

It is evident from Figure 5 that the shape of the C/N_0 profile is largely determined by the transmit antenna pattern. The GOES-16 scenario, with its relatively constant altitude, provides a good opportunity to validate this aspect of the simulation. Using the C/N_0 from the flight data and the simulated geometry and receiver parameters, it is possible to calculate the measured transmit antenna gain:

$$G_T = C/N_0 - P_T - G_R - A_d + (T_s + k + Nf). \quad (2)$$

This will include, of course, any additional errors in the simulation besides the transmit antenna patterns. The calculated patterns are overlaid on the reference patterns in Figure 6, where all azimuth cuts are plotted together. The main lobes match well, as do the first sidelobe for some blocks, though the flight data clearly shows azimuthal variation for the IIF block that is not captured in the mean IIA pattern being used.

Verification With MMS Flight Data

In early 2017, the MMS spacecraft transitioned to Phase 2, highly elliptical orbits with apogee altitudes around 153,000 km. This is the highest altitude, operational use of on-board, GPS-based

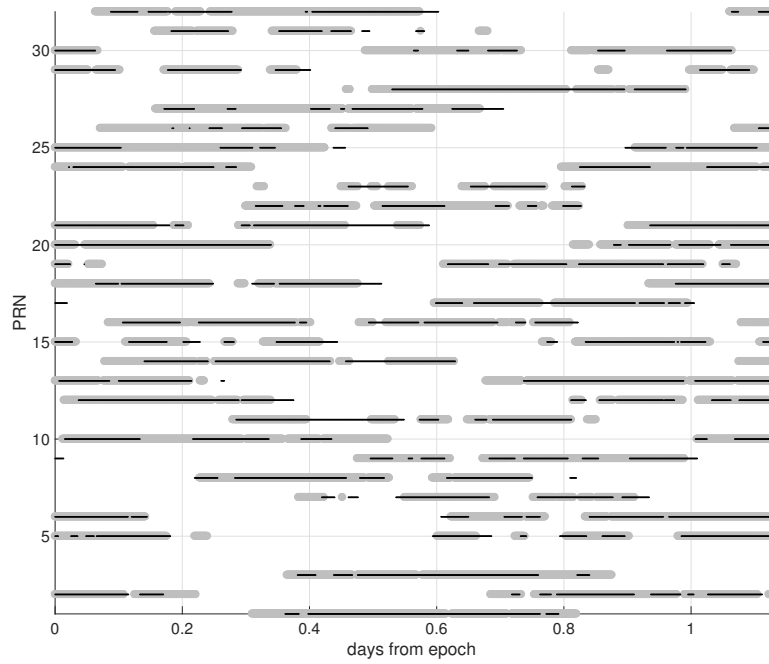


Figure 4. GOES-16 GPS visibility per SV - simulation (grey) and flight data (black).

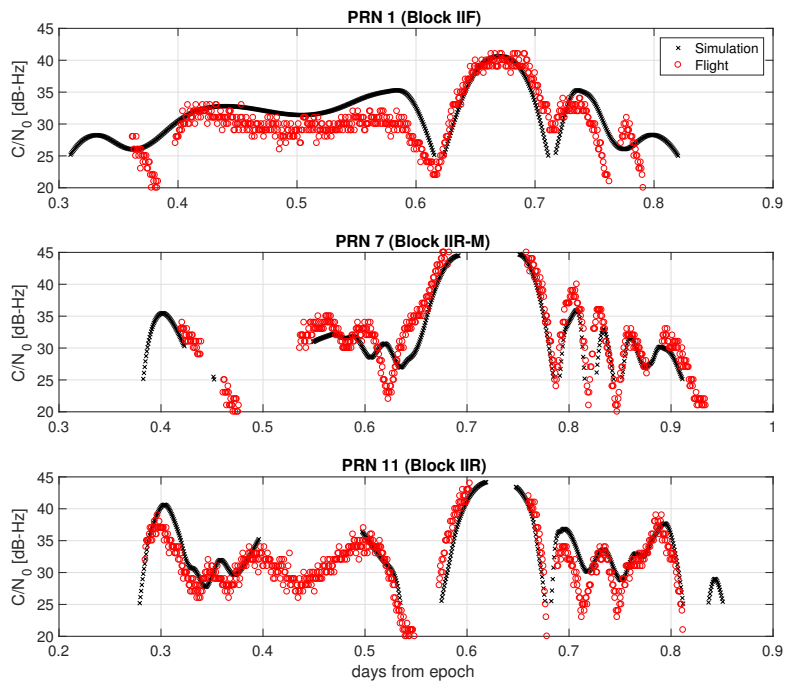


Figure 5. GOES-16 received C/N_0 for PRNs 1, 7, and 11.

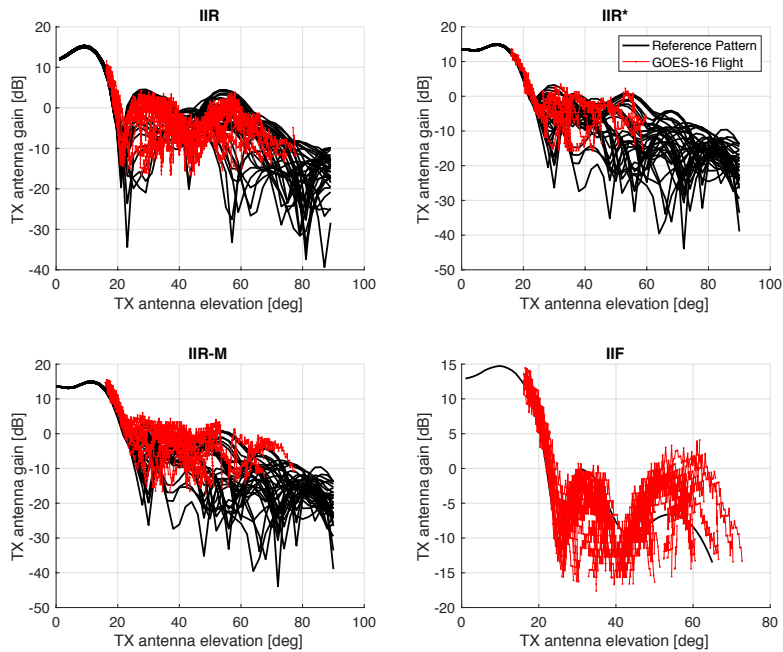


Figure 6. Comparison between GPS transmit antenna patterns computed from GOES-16 data and simulated patterns.

navigation, and is used here to assess the ODTBX simulation of satellite visibility beyond the formal limit of the SSV. Navigation results for this phase of the MMS mission have been previously presented,¹⁸ demonstrating an average of three signals tracked near apogee (and sometimes as many as eight), with at least one satellite tracked 99% of the time and four or more tracked 70% of the time.

We used a trajectory from the MMS team for one of the spacecraft, starting May 22, 2017 with a duration of eight days, approximately two complete orbits. As in Winternitz¹⁸ (2017), we used an azimuthally symmetric antenna to account for the spacecraft spin and multiple on-board antennas. This antenna approximation is pointed toward ecliptic north, with a 7 dB peak gain at 90°, essentially forming a belt of gain around the spacecraft, parallel to the ecliptic and perpendicular to the spin axis. We modeled the 12-channel GPS receiver with an acquisition and tracking threshold of 22 dB-Hz, again according to inspection of the flight data.

Intervals when each SV was visible over the duration of the simulation are shown in Figure 7, with flight data results overlaid in black. Here again, the simulation and flight data broadly agree, though in general the simulation registers more visibility and fewer outages than recorded in the flight data. As with GOES-16, the individual C/N_0 profiles for each SV match the main lobe measurements better than sidelobes, which account for most of the discrepancies observed in Figure 7. This is consistent with the simulation results in Winternitz¹⁸ (2017).

Our focus with the MMS scenario, however, was on the number of signals visible over altitude, as this is the key metric in the lunar simulation. This is shown in Figure 8 for both MMS and GOES-16, where the visibility number is binned by altitude increments of Earth radii ($R_E = 6378.14$ km) and averaged. For example, the MMS point at $1R_E$ indicates that an average of 12 SVs were

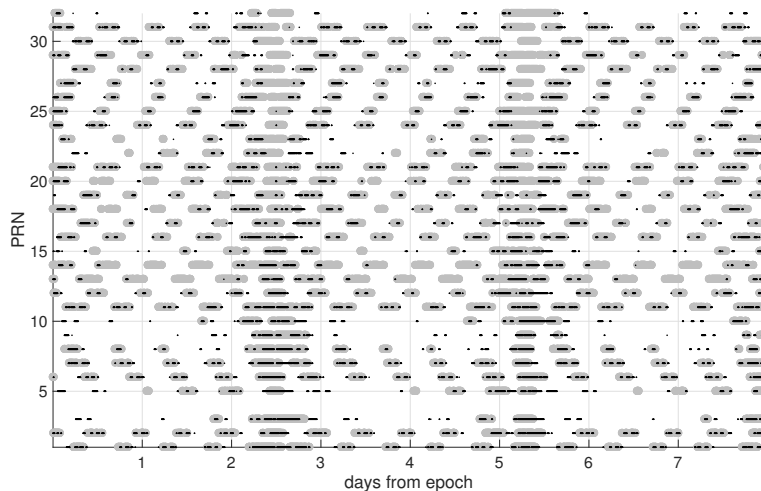


Figure 7. MMS GPS visibility per SV - simulation (grey) and flight data (black).

visible between 0 and $1R_E$. An abundance of signals are available past the GPS constellation at approximately $3.2R_E$ and well beyond the formal limit of the SSV at approximately $5.6R_E$. The simulation is consistent with the flight results, but shows slightly higher availability beyond $20R_E$.

LUNAR DESIGN REFERENCE MISSIONS

The United States plans to return to human exploration of the Moon and cislunar space in the next few years with the first two Exploration Missions, EM-1 and EM-2. These missions re-establish the fundamental capabilities necessary to take humans from the Earth, to cislunar space, and back again, first with an un-crewed distant retrograde orbit (DRO) with EM-1, then with a crewed, free-return trajectory with EM-2.³ Long-term plans are still under development, but the Deep Space Gateway is one objective—a permanent way-station in the vicinity of the moon for training and staging for deep space activity.⁴ An Near Rectilinear Halo Orbit (NRHO) is one proposed orbit;³² this is the orbit considered here, shown in Figure 9. For simplicity, we only show the outbound cruise and first half of the NRHO, as the inbound cruise had identical visibility results.

We simulated three different configurations for the lunar mission. The first, for purposes of validation, used the same receiver characteristics (i.e., 22 dB-Hz acquisition and tracking threshold) and antenna pattern as the MMS simulation. The second configuration used the same 22 dB-Hz acquisition and tracking threshold, but with an Earth-pointed, high gain antenna. We simulated two antenna cases - 10 dB and 14 dB peak gain. Finally, we simulated a case with a 1 dB threshold and the same high gain antenna, in order to provide a baseline for receiver design trade studies. We simulated all three cases at the May 22, 2017 epoch of the MMS mission in order to avoid any errors in forward propagating the GPS constellation.

RESULTS

The number of SVs visible over altitude is shown in Figure 10. MMS flight data is also shown, and visibility numbers are consistent for the lunar case with the same receiver parameters during the period of overlap. Beyond the MMS altitude, signal availability for this case drops below 4 SVs,

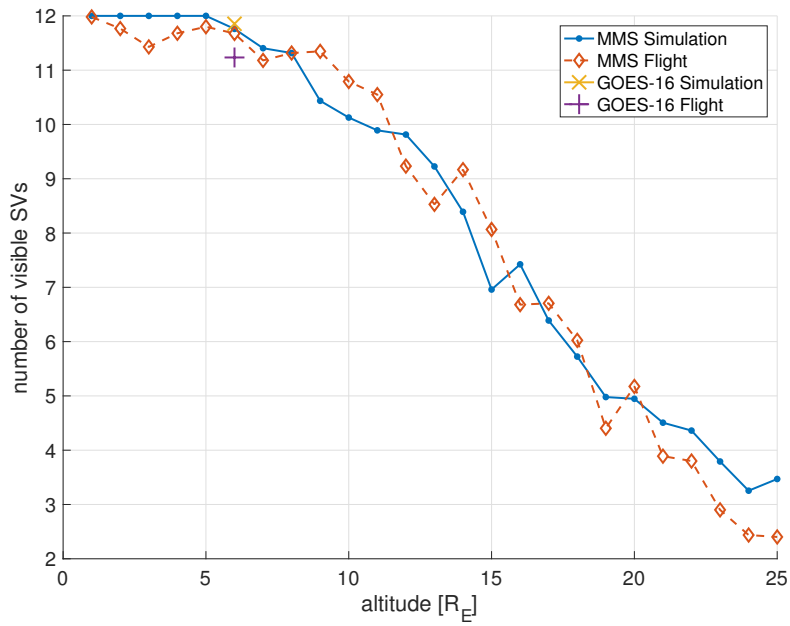


Figure 8. MMS and GOES-16: number of SVs visible over altitude, averaged in increments of R_E .

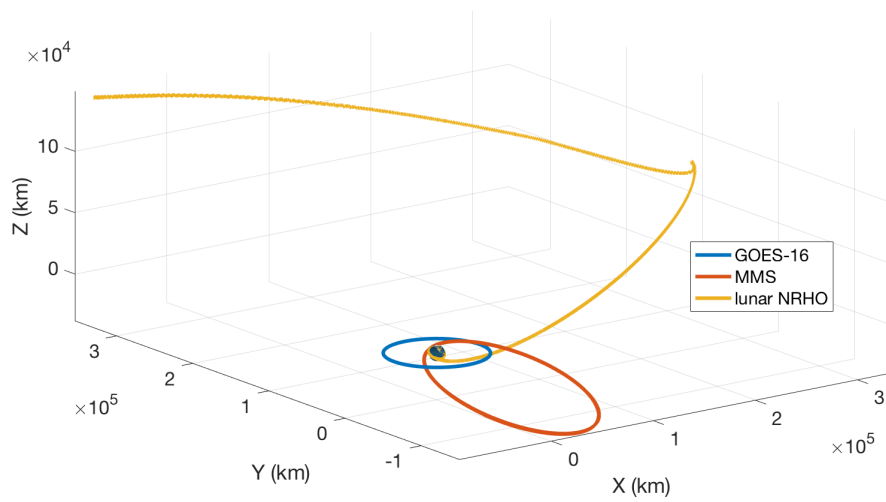


Figure 9. Orbits simulated in this study: GOES-16, MMS, and a lunar NRHO.

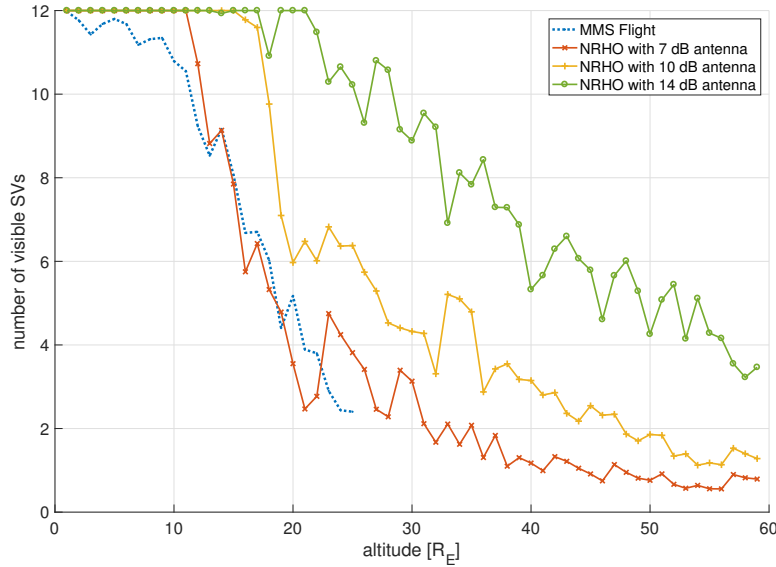


Figure 10. Lunar trajectory: number of SVs visible over altitude, averaged in increments of R_E .

and continues to decline until an average of only one signal is available. Four or more signals are visible for 8% of the trajectory, one or more for 68% of the time, and the longest outage is 140 minutes.

Adding the 10 dB high gain antenna extends the possibility of 4+ signals beyond $30R_E$ —halfway to the Moon, and an important point for mid-course correction burns. In this case, four or more signals are available for 17% of the trajectory, one or more for 82%. The maximum outage is 84 minutes. An antenna with a peak gain of 10 dB is typical for the lunar studies discussed previously, but gain several dB higher is feasible.²⁴ The Winternitz¹⁸ paper extending MMS Phase 2 results to the Moon used a 14 dB antenna and the same NRHO trajectory we used here. Our 14 dB case is consistent with their results: the possibility of three or more signals at the Moon, one or more signals for 99% of the trajectory, four or more signals 65% of the trajectory, and a maximum outage of only 11 minutes.

In addition to antenna gain, receiver sensitivity is a design element critically important to GPS-based navigation at lunar distances. Weak signal tracking was an enabling feature of the Navigator GPS receiver in the case of MMS, and is the focus of much of the GNSS receiver development specific to lunar applications. Through the use of Galileo pilot channels, on-board inertial sensors, and other means, receiver designers are pursuing acquisition and tracking thresholds at or below 10 dB-Hz.^{24,33} In Figure 11, the number of visible signals is shown as a function of both receiver threshold and altitude for the lunar NRHO. A receiver with an acquisition threshold of 25 dB-Hz, for instance, would not acquire any signals at lunar distances. A threshold of around 15 dB-Hz or lower would be required to acquire, on average, more than one signal at lunar distances.

CONCLUSION

We have used newly-available knowledge of the GPS constellation, including high-resolution antenna gain patterns released for the Block IIR and IIR-M satellites, and on-orbit data from GOES-16

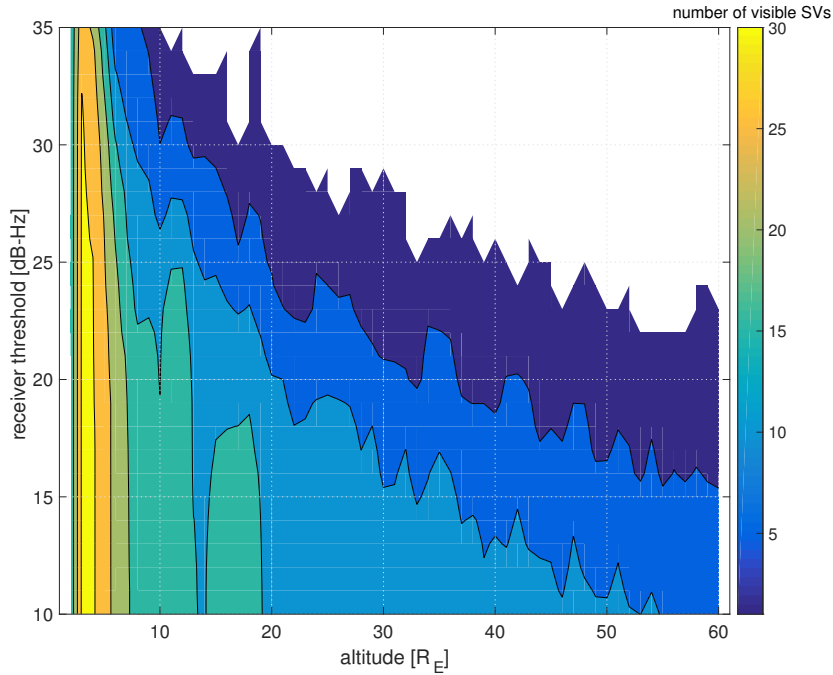


Figure 11. Number of satellites visible as a function of altitude and receiver C/N_0 threshold.

Table 2. Outbound lunar NRHO visibility with 22 dB-Hz acquisition/tracking threshold.

Peak Antenna Gain	1+	4+	Maximum Outage
7 dB	63%	8%	140 min
10 dB	82%	17%	84 min
14 dB	99%	65%	11 min

and MMS, to update our knowledge of the expected GPS signal availability that can be obtained at lunar distances. At altitudes as high as $25R_E$, the available models provide consistency between our simulated visibility and the available flight data to within a few percent in overall visibility metrics. Based on this validation, we demonstrated the visibility metrics shown in Table 2 for different antennas. By utilizing receiver sensitivity improvements that allow for tracking at the 15 dB-Hz level, consistent availability of 5 or more GPS signals simultaneously can be achieved. However, comparable performance can be achieved with existing receiver technology and a 14 dB antenna, thereby avoiding the higher navigation message bit errors that arise from extreme weak signal tracking.

Continuous or nearly-continuous availability of GPS in lunar-vicinity orbits has profound implications for lunar navigation architectures in the future, including NASA's upcoming Exploration Missions and the DSG. Such measurements alone can provide accurate navigation solutions during outbound and return mission phases, and can play a significant role as part of a larger navigation architecture despite the poor geometry. Once initialized, perhaps via occasional ground-based ranging contacts, only sporadic GPS measurements are required to maintain an accurate navigation solution in an on-board navigation filter, and only one occasional GPS signal is required to maintain accurate

onboard time. Furthermore, the availability of continuous measurements allows for more rapid stationkeeping using electric propulsion, without placing additional burden the ground-based ranging networks.

This paper outlines a baseline capability in terms of GPS signal availability alone. A modest amount of additional gain or sensitivity was shown to increase coverage significantly, underscoring the importance of high fidelity modeling. Future work must translate this availability to mission-level navigation performance analysis, considering the effects of Dilution of Precision (DOP) for candidate missions of interest as part of a complete navigation architecture. Additionally, efforts are underway through the United Nations (UN) International Committee on GNSS (ICG) to formalize and document the multi-GNSS SSV, a concept that reflects the combined high-altitude capability of all six global and regional GNSS constellations. Further study is required to extend the results of this paper to the new multi-GNSS environment.

REFERENCES

- [1] J. N. Goswami and M. Annadurai, "Chandrayaan-2 Mission," *Lunar and Planetary Science Conference*, Vol. 42 of *Lunar and Planetary Inst. Technical Report*, Mar. 2011, p. 2042.
- [2] Q. Wang and J. Liu, "A Chang'e-4 Mission Concept and Vision of Future Chinese Lunar Exploration Activities," *Acta Astronautica*, Vol. 127, 2016, pp. 678 – 683, <https://doi.org/10.1016/j.actaastro.2016.06.024>.
- [3] J. P. Gutkowski, T. F. Dawn, and R. M. Jedrey, "Evolution of Orion Mission Design for Exploration Mission 1 and 2," *Annual AAS Guidance, Navigation and Control Conference*, Feb 2016.
- [4] "Deep Space Gateway to Open Opportunities for Distant Destinations," <https://www.nasa.gov/feature/deep-space-gateway-to-open-opportunities-for-distant-destinations>, March 2017.
- [5] "Presidential Memorandum on Reinvigorating America's Human Space Exploration Program," <https://www.whitehouse.gov/presidential-actions/presidential-memorandum-reinvigorating-americas-human-space-exploration-program/>, December 2017.
- [6] O. Balbach, B. Eissfeller, G. Hein, T. Zink, W. Enderle, M. Schmidhuber, , and N. Lemke, "Tracking GPS above GPS Satellite Altitude: Results of the GPS Experiment on the HEO Mission Equator-S," *Proceedings of the 9th International Technical Meeting of the Satellite Division of The Institute of Navigation (ION GPS 1996)*, Nashville, TN, September 1998.
- [7] T. Powell, P. D. Martzen, S. Sedlacek, C. Chao, R. Silva, A. Brown, and G. Belle, "GPS Signals in a Geosynchronous Transfer Orbit: Falcon Gold Data Processing," *Proceedings of the Institute of Navigation National Technical Meeting*, January 1999, pp. 575–585.
- [8] J. Kronman, "Experience Using GPS For Orbit Determination of a Geosynchronous Satellite," *Proceedings of the Institute of Navigation GPS*, Salt Lake City, UT, September 2000.
- [9] M. C. Moreau, F. H. Bauer, J. R. Carpenter, E. P. Davis, G. W. Davis, , and L. A. Jackson, "Preliminary Results of the GPS Flight Experiment on the High Earth Orbit AMSAT-OSCAR 40 Spacecraft," *Proceedings of AAS Guidance and Control Conference*, Breckenridge, CO, February 2002.
- [10] G. Davis, M. Moreau, J. Carpenter, and F. Bauer, "GPS-Based Navigation and Orbit Determination for the AMSAT AO-40 Satellite," *Proceedings of the Guidance, Navigation, and Control Conference*, Reston, VA, August 2002.
- [11] F. Bauer, M. Moreau, M. Dahle-Melsaether, W. Petrofski, B. Stanton, S. Thomason, G. Harris, R. Sena, and L. T. III, "The GPS Space Service Volume," *Proceedings of the 19th International Technical Meeting of the Satellite Division of The Institute of Navigation (ION GNSS 2006)*, 2006, pp. 2503–2514.
- [12] M. Unwin, R. D. Van Steenwijk, P. Blunt, Y. Hashida, S. Kowaltschek, and L. Nowak, "Navigating Above the GPS Constellation - Preliminary Results from the SGR-GEO on GIOVE-A," *Proceedings of the 26th International Technical Meeting of The Satellite Division of the Institute of Navigation (ION GNSS+ 2013)*, 2013, pp. 3305–3315.
- [13] G. Verde, M. Unwin, S. Duncan, A. Hyslop, and S. Kowaltschek, "Revisiting the SGR-GEO on GIOVE-A for GPS Satellite Antenna Pattern Mapping," *Proceedings of the 10th International ESA Conference on Guidance, Navigation and Control Systems*, Salzburg, Austria, European Space Agency, May 2017.
- [14] F. Bauer, J. Parker, B. Welch, and W. Enerle, "Developing a Robust, Interoperable GNSS Space Service Volume (SSV) for the Global Space User Community," *Proceedings of the 2017 International Technical Meeting of the Institute of Navigation*, Monterey, CA, January 2017.

- [15] L. Winternitz, M. Moreau, G. Boegner, and S. Sirotzky, "Navigator GPS Receiver for Fast Acquisition and Weak Signal Space Applications," *Proceedings of the Institute of Navigation GNSS 2004 Conference*, Long Beach, CA, Institute of Navigation, September 2004.
- [16] L. Winternitz, W. Bamford, S. Price, J. Carpenter, A. Long, and M. Farahmand, "Global Positioning System Navigation Above 76,000 km for NASA's Magnetospheric Multiscale Mission," *AAS GN&C Conference*, Breckenridge, CO, American Astronautical Society, February 2016.
- [17] S. Winkler, G. Ramsey, C. Frey, J. Chapel, D. Chu, D. Freesland, A. Krimchansky, and M. Concha, "GPS Receiver On-Orbit Performance for the GOES-R Spacecraft," *Proceedings of the 10th International ESA Conference on Guidance, Navigation and Control Systems*, Salzburg, Austria, European Space Agency, May 2017.
- [18] L. B. Winternitz, W. A. Bamford, and S. R. Price, "New High-Altitude GPS Navigation Results from the Magnetospheric Multiscale Spacecraft and Simulations at Lunar Distances," *Proceedings of the 30th International Technical Meeting of The Satellite Division of the Institute of Navigation (ION GNSS+ 2017)*, Portland, OR, Institute of Navigation, September 2017.
- [19] G. Barton, S. Sheppard, and T. Brand, "Proposed Autonomous Lunar Navigation System," *Proceedings of AAS Guidance and Control Conference*, Breckenridge, CO, February 1993.
- [20] J. Carpenter, D. Folta, M. Moreau, and D. Quinn, "Libration Point Navigation Concepts Supporting the Vision for Space Exploration," *AIAA/AAS Specialist Conference*, Providence, RI, August 2004.
- [21] W. Bamford, G. Heckler, G. Holt, and M. Moreau, "A GPS Receiver for Lunar Missions," *Proceedings of the 2008 National Technical Meeting of The Institute of Navigation*, San Diego, CA, January 2008.
- [22] L. Winternitz, W. Bamford, and G. Heckler, "A GPS Receiver for High Altitude Satellite Navigation," *IEEE Journal of Selected Topics in Signal Processing*, Vol. 3, No. 4, 2009.
- [23] T. Lee, A. Long, K. Berry, J. Carpenter, M. Moreau, and G. Holt, "Navigating the Return Trip from the Moon Using Earth-Based Ground Tracking and GPS," *Proceedings of AAS Guidance and Control Conference*, Breckenridge, CO, February 2009.
- [24] N. Witternigg, G. Obertaxer, M. Schoenhuber, G. Palmerini, F. Rodriguez, L. Capponi, F. Soualle, and J. Floch, "Weak GNSS Signal Navigation for Lunar Exploration Missions," *Proceedings of the 28th International Technical Meeting of The Satellite Division of the Institute of Navigation (ION GNSS+ 2015)*, Tampa, FL, Institute of Navigation, September 2015.
- [25] V. Capuano, C. Botteron, J. Leclare, J. Tian, Y. Wang, and P. Farine, "Feasibility Study of GNSS as Navigation Systems to Reach the Moon," *Acta Astronautica*, July 2015.
- [26] E. Shehaj, V. Capuano, C. Botteron, P. Blunt, and P. Farine, "GPS Based Navigation Performance Analysis Within and Beyond the Space Service Volume for Different Transmitters? Antenna Patterns," *MDPI Aerospace*, Vol. 4, August 2017, pp. 1–34.
- [27] "Orbit Determination Toolbox (ODTBX) 6.5," <http://opensource.gsfc.nasa.gov/projects/ODTBX/>, January 2017.
- [28] "GPS Block IIR/IIR-M Antenna Panel Data," <http://www.lockheedmartin.com/us/products/gps/gps-publications.html>. Lockheed Martin Corporation.
- [29] F. M. Czopek and S. Shollenberger, "Description and Performance of the GPS Block I and II L-Band Antenna and Link Budget," *Proceedings of the 6th International Technical Meeting of the Satellite Division of The Institute of Navigation (ION GPS 1993)*, Institute of Navigation, 1993, pp. 37–43.
- [30] J. J. K. Parker, J. E. Valdez, F. H. Bauer, and M. C. Moreau, "Use and Protection of GPS Sidelobe Signals for Enhanced Navigation Performance in High Earth Orbit," *Proceedings of the 39th Annual AAS Guidance and Control Conference*, Breckenridge, CO, American Astronautical Society, February 2016.
- [31] Y. E. Bar-Sever, "A New Model for Yaw Attitude of Global Positioning System Satellites," Report TDA Progress Report 42-123, Jet Propulsion Laboratory, 1995.
- [32] J. Carpenter, "ESA Workshop: Research Opportunities on the Deep Space Gateway," Tech. Rep. ESA-HSO-K-AR-0000, European Space Agency, 2017.
- [33] L. Musumeci, F. Dovis, J. a. S. Silva, P. F. da Silva, and H. D. Lopes, "Design of a High Sensitivity GNSS Receiver for Lunar missions," *Advances in Space Research*, Vol. 57, June 2016, pp. 2285–2313.